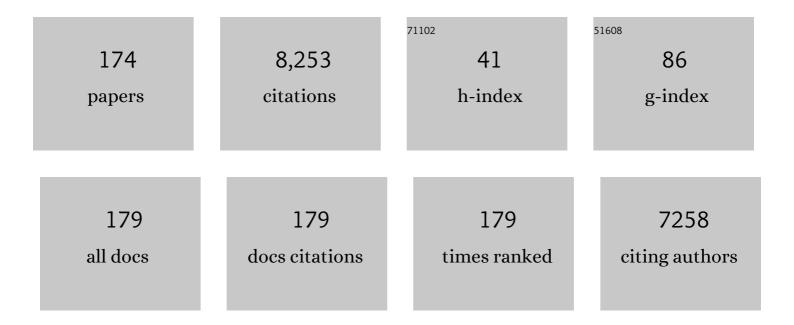
## Peter R Slater

List of Publications by Year in descending order

Source: https://exaly.com/author-pdf/5401583/publications.pdf Version: 2024-02-01



DETED D SIATED

#	Article	IF	CITATIONS
1	Assessing the Importance of Cation Size in the Tetragonal ubic Phase Transition in Lithiumâ€Garnet Electrolytes**. Chemistry - A European Journal, 2022, 28, .	3.3	5
2	High entropy lithium garnets – Testing the compositional flexibility of the lithium garnet system. Journal of Solid State Chemistry, 2022, 308, 122944.	2.9	10
3	Halogenation of Li <sub>7</sub> La <sub>3</sub> Zr <sub>2</sub> O <sub>12</sub> solid electrolytes: a combined solid-state NMR, computational and electrochemical study. Journal of Materials Chemistry A, 2022, 10, 11172-11185.	10.3	6
4	High-Voltage Stabilization of O3-Type Layered Oxide for Sodium-Ion Batteries by Simultaneous Tin Dual Modification. Chemistry of Materials, 2022, 34, 4153-4165.	6.7	47
5	Synthesis and structure of the perovskite related Sr4-xBaxNa1-yLiy(BO3)3 solid solution series and the related a site cation ordered (Sr/Ca)4Li(BO3)3 system. Journal of Solid State Chemistry, 2021, 294, 121870.	2.9	0
6	Evaluation of Ga <sub>0.2</sub> Li <sub>6.4</sub> Nd <sub>3</sub> Zr <sub>2</sub> O <sub>12</sub> garnets: exploiting dopant instability to create a mixed conductive interface to reduce interfacial resistance for all solid state batteries. Dalton Transactions, 2021, 50, 13786-13800.	3.3	6
7	Raman spectroscopy insights into the α- and δ-phases of formamidinium lead iodide (FAPbI <sub>3</sub> ). Dalton Transactions, 2021, 50, 3315-3323.	3.3	12
8	Water based synthesis of highly conductive GaxLi7â^'3xLa3Hf2O12 garnets with comparable critical current density to analogous GaxLi7â^'3xLa3Zr2O12 systems. Dalton Transactions, 2021, 50, 2364-2374.	3.3	6
9	Carbon dioxide decomposition through gas exchange in barium calcium iron niobates. Catalysis Today, 2021, 364, 211-219.	4.4	6
10	Structural, Magnetic and Catalytic Properties of a New Vacancy Ordered Perovskite Type Barium Cobaltate BaCoO <sub>2.67</sub> . Chemistry - A European Journal, 2021, 27, 9763-9767.	3.3	6
11	Electrochemical Reduction and Oxidation of Ruddlesden–Popper-Type La <sub>2</sub> NiO <sub>3</sub> F <sub>2</sub> within Fluoride-Ion Batteries. Chemistry of Materials, 2021, 33, 499-512.	6.7	19
12	Topochemical Fluorination of n = 2 Ruddlesden–Popper Type Sr3Ti2O7 to Sr3Ti2O5F4 and Its Reductive Defluorination. Inorganic Chemistry, 2020, 59, 1153-1163.	4.0	12
13	Combined Experimental and Computational Study of Ce-Doped La <sub>3</sub> Zr <sub>2</sub> Li <sub>7</sub> O <sub>12</sub> Garnet Solid-State Electrolyte. Chemistry of Materials, 2020, 32, 215-223.	6.7	40
14	Suitability of strontium and cobalt-free perovskite cathodes with La9.67Si5AlO26 apatite electrolyte for intermediate temperature solid oxide fuel cells. Dalton Transactions, 2020, 49, 14280-14289.	3.3	2
15	X-ray pair distribution function analysis and electrical and electrochemical properties of cerium doped Li <sub>5</sub> La <sub>3</sub> Nb <sub>2</sub> O <sub>12</sub> garnet solid-state electrolyte. Dalton Transactions, 2020, 49, 11727-11735.	3.3	10
16	Carbon dioxide and water incorporation mechanisms in SrFeO <sub>3â^îÎ</sub> phases: a computational study. Physical Chemistry Chemical Physics, 2020, 22, 25146-25155.	2.8	4
17	Evaluation of the effect of site substitution of Pr doping in the lithium garnet system Li <sub>5</sub> La <sub>3</sub> Nb <sub>2</sub> N2 <sub>12</sub> . Dalton Transactions, 2020, 49, 10349-10359.	3.3	10
18	Investigation of PO43â^' oxyanion-doping on the properties of CaFe0.4Ti0.6O3â^'δ for potential application as symmetrical electrodes for SOFCs. Journal of Alloys and Compounds, 2020, 835, 155437.	5.5	9

#	Article	IF	CITATIONS
19	The Building Blocks of Battery Technology: Using Modified Tower Block Game Sets to Explain and Aid the Understanding of Rechargeable Li-Ion Batteries. Journal of Chemical Education, 2020, 97, 2231-2237.	2.3	8
20	Understanding the effect of water transport on the thermal expansion properties of the perovskites BaFe0.6Co0.3Nb0.1O3ⴴδ and BaCo0.7Yb0.2Bi0.1O3â´`δ. Journal of Materials Science, 2020, 55, 13590-13604.	3.7	1
21	Synthesis, structure and electrochemical performance of Eldfellite, NaFe(SO4)2, doped with SeO4, HPO4 and PO3F. Journal of Solid State Chemistry, 2020, 289, 121395.	2.9	6
22	Topochemical Reduction of La <sub>2</sub> NiO <sub>3</sub> F <sub>2</sub> : The First Ni-Based Ruddlesden–Popper <i>n</i> = 1 T′-Type Structure and the Impact of Reduction on Magnetic Ordering. Chemistry of Materials, 2020, 32, 3160-3179.	6.7	19
23	Degradation induced lattice anchoring self-passivation in CsPbI <sub>3â^'x</sub> Br <sub>x</sub> . Journal of Materials Chemistry A, 2020, 8, 9963-9969.	10.3	7
24	Low temperature synthesis of garnet solid state electrolytes: Implications on aluminium incorporation in Li7La3Zr2O12. Solid State Ionics, 2020, 350, 115317.	2.7	17
25	Comparison of the thermal resistance behaviour of synthesized Ln4Al2O9 (Lnâ€=â€Y, Sm, Eu, Gd, Tb) materials vs commercial Zr0.8Y0.2O1.9 (8YSZ). Surface and Coatings Technology, 2019, 374, 745-751.	4.8	4
26	Effect of Si-Doping on the Structure and Conductivity of (Sr/Ca)2MnFeO6-δSystems. ECS Transactions, 2019, 91, 1425-1436.	0.5	2
27	Introduction of Sulfate to Stabilize the n = 3 Ruddlesden-Popper System Sr4Fe3O10-δ, as a Potential SOFC Cathode. ECS Transactions, 2019, 91, 1467-1476.	0.5	4
28	BaCoO <sub>2+δ</sub> : a new highly oxygen deficient perovskite-related phase with unusual Co coordination obtained by high temperature reaction with short reaction times. Chemical Communications, 2019, 55, 2920-2923.	4.1	3
29	Recycling lithium-ion batteries from electric vehicles. Nature, 2019, 575, 75-86.	27.8	1,699
30	Synthesis of new Ln <sub>4</sub> (Al <sub>2</sub> O <sub>6</sub> F <sub>2</sub> )O <sub>2</sub> (Ln =) Tj ETQ	2q0,0 0 rg 2,2	BT /Overloc
31	Mechanism of Carbon Dioxide and Water Incorporation in Ba2TiO4: A Joint Computational and Experimental Study. Journal of Physical Chemistry C, 2018, 122, 1061-1069.	3.1	4
32	Structure and Lithium-Ion Dynamics in Fluoride-Doped Cubic Li <sub>7</sub> La <sub>3</sub> Zr <sub>2</sub> O <sub>12</sub> (LLZO) Garnet for Li Solid-State Battery Applications. Journal of Physical Chemistry C, 2018, 122, 27811-27819.	3.1	36
33	Designing a facile low cost synthesis strategy for the Na–V–S–O systems, NaV(SO <sub>4</sub> ) <sub>2</sub> , Na <sub>3</sub> V(SO <sub>4</sub> ) <sub>3</sub> and Na <sub>2</sub> VO(SO <sub>4</sub> ) <sub>2</sub> . Dalton Transactions, 2018, 47, 13535-13542.	3.3	12
34	Synthesis, structure and electrical conductivity of a new perovskite type barium cobaltate BaCoO <sub>1.80</sub> (OH) <sub>0.86</sub> . Dalton Transactions, 2018, 47, 11136-11145.	3.3	10
35	Topochemical Fluorination of La2NiO4+d: Unprecedented Ordering of Oxide and Fluoride lons in La2NiO3F2. Inorganic Chemistry, 2018, 57, 6549-6560.	4.0	30
36	Carbonate: an alternative dopant to stabilize new perovskite phases; synthesis and structure of Ba <sub>3</sub> Yb <sub>2</sub> O <sub>5</sub> CO <sub>3</sub> and related isostructural phases Ba <sub>3</sub> Ln <sub>2</sub> O <sub>5</sub> CO <sub>3</sub> (Ln = Y, Dy, Ho, Er, Tm and Lu). Dalton Transactions, 2018, 47, 12901-12906.	3.3	6

#	Article	IF	CITATIONS
37	Thermochemical CO <sub>2</sub> splitting using double perovskite-type Ba <sub>2</sub> Ca <sub>0.66</sub> Nb <sub>1.34â°`x</sub> Fe <sub>x</sub> O <sub>6â~`δ</sub> . Journal of Materials Chemistry A, 2017, 5, 6874-6883.	10.3	23
38	Investigation into the Effect of Sulfate and Borate Incorporation on the Structure and Properties of SrFeO3-1´. Crystals, 2017, 7, 169.	2.2	8
39	Large Nonclassical Electrostriction in (Y, Nb)â€Stabilized <i>δ</i> â€Bi <sub>2</sub> O <sub>3</sub> . Advanced Functional Materials, 2016, 26, 1138-1142.	14.9	50
40	Magnetic interactions in cubic-, hexagonal- and trigonal-barium iron oxide fluoride, BaFeO <sub>2</sub> F. Journal of Physics Condensed Matter, 2016, 28, 346001.	1.8	6
41	A computational study of doped olivine structured Cd <sub>2</sub> GeO <sub>4</sub> : local defect trapping of interstitial oxide ions. Physical Chemistry Chemical Physics, 2016, 18, 26284-26290.	2.8	5
42	Exploring the mixed transport properties of sulfur( <scp>vi</scp> )-doped Ba <sub>2</sub> In <sub>2</sub> O <sub>5</sub> for intermediate-temperature electrochemical applications. Journal of Materials Chemistry A, 2016, 4, 11069-11076.	10.3	9
43	Effect of tri- and tetravalent metal doping on the electrochemical properties of lanthanum tungstate proton conductors. Dalton Transactions, 2016, 45, 3130-3138.	3.3	13
44	Neutron diffraction and multinuclear solid state NMR investigation into the structures of oxide ion conducting La <sub>9.6</sub> Si <sub>6</sub> O <sub>26.4</sub> and La <sub>8</sub> Sr <sub>2</sub> Si <sub>6</sub> O <sub>26</sub> , and their hydrated phases. Dalton Transactions, 2016, 45, 121-133.	3.3	9
45	Interstitial Oxide Ion Distribution and Transport Mechanism in Aluminum-Doped Neodymium Silicate Apatite Electrolytes. Journal of the American Chemical Society, 2016, 138, 4468-4483.	13.7	12
46	Synthesis, structural characterisation and proton conduction of two new hydrated phases of barium ferrite BaFeO <sub>2.5â^'x</sub> (OH) <sub>2x</sub> . Journal of Materials Chemistry A, 2016, 4, 3415-3430.	10.3	16
47	Oxyanions in perovskites: from superconductors to solid oxide fuel cells. Dalton Transactions, 2015, 44, 10559-10569.	3.3	39
48	Laser machining of LaNi0.6M0.4O3â~δ (M: Co, Fe) dip-coated on a Fe–22Cr mesh material to obtain aÂnew contact coating for SOFC: Interaction between Crofer22APU interconnect and La0.6Sr0.4FeO3 cathode. International Journal of Hydrogen Energy, 2015, 40, 8407-8418.	7.1	12
49	Reply to "Structural and magnetic behavior of the cubic oxyfluoride SrFeO2F studied by neutron diffraction― Journal of Solid State Chemistry, 2015, 226, 326-331.	2.9	10
50	Anisotropic oxide ion conduction in melilite intermediate temperature electrolytes. Journal of Materials Chemistry A, 2015, 3, 3091-3096.	10.3	25
51	Synthesis and characterization of novel Ge doped Sr 1â^'y Ca y FeO 3â^'î´ SOFC cathode materials. Materials Research Bulletin, 2015, 67, 63-69.	5.2	6
52	Crystal Chemical Analysis of Nd <sub>9.33</sub> Si <sub>6</sub> O <sub>26</sub> and Nd <sub>8</sub> Sr <sub>2</sub> Si <sub>6</sub> O <sub>26</sub> Apatite Electrolytes Using Aberration-Corrected Scanning Transmission Electron Microscopy and Impedance Spectroscopy. Chemistry of Materials, 2015, 27, 1217-1222.	6.7	8
53	Evaluation of using protective/conductive coating on Fe-22Cr mesh as a composite cathode contact material for intermediate solid oxide fuel cells. International Journal of Hydrogen Energy, 2015, 40, 4804-4818.	7.1	19
54	A combined single crystal neutron/X-ray diffraction and solid-state nuclear magnetic resonance study of the hybrid perovskites CH <sub>3</sub> NH <sub>3</sub> PbX <sub>3</sub> (X = I, Br and Cl). Journal of Materials Chemistry A, 2015, 3, 9298-9307.	10.3	253

#		Article	IF	CITATIONS
58	5	Metallic/Ceramic (Fe-22Cr mesh/ LaNi0.6Fe0.4O3-Â) Composite as Contact Material for SOFCs. ECS Transactions, 2015, 68, 1701-1706.	0.5	1
56	6	Perovskite-Related Oxide Fluorides: The Use of Mössbauer Spectroscopy in the Investigation of Magnetic Properties. Croatica Chemica Acta, 2015, 88, 339-346.	0.4	0
57	7	Investigation into the effect of Si doping on the cell symmetry and performance of Sr1â^'yCayFeO3â^'δ SOFC cathode materials. Journal of Solid State Chemistry, 2014, 213, 132-137.	2.9	22
58	8	Introducing a Large Polar Tetragonal Distortion into Ba-Doped BiFeO <sub>3</sub> by Low-Temperature Fluorination. Inorganic Chemistry, 2014, 53, 12572-12583.	4.0	29
59	9	Development of CaMn <sub>1â^'x</sub> Ru <sub>x</sub> O <sub>3â^'y</sub> (x = 0 and 0.15) oxygen reduction catalysts for use in low temperature electrochemical devices containing alkaline electrolytes: ex situ testing using the rotating ring-disk electrode voltammetry method. Journal of Materials Chemistry A. 2014. 2, 3047-3056.	10.3	37
60	0	Structural Study of the Apatite Nd <sub>8</sub> Sr <sub>2</sub> Si <sub>6</sub> O <sub>26</sub> by Laue Neutron Diffraction and Single-Crystal Raman Spectroscopy. Inorganic Chemistry, 2014, 53, 9416-9423.	4.0	7
61	1	LaNi0.6Co0 4O3â^' dip-coated on Fe–Cr mesh as a composite cathode contact material on intermediate solid oxide fuel cells. Journal of Power Sources, 2014, 269, 509-519.	7.8	19
62		Crystallographic and Magnetic Structure of the Perovskite-Type Compound BaFeO <sub>2.5</sub> : Unrivaled Complexity in Oxygen Vacancy Ordering. Inorganic Chemistry, 2014, 53, 5911-5921.	4.0	44
63	3	Hydrothermal Synthesis, Structure Investigation, and Oxide Ion Conductivity of Mixed Si/Ge-Based Apatite-Type Phases. Inorganic Chemistry, 2014, 53, 4803-4812.	4.0	14
64		Investigation into the Incorporation of Phosphate into BaCe1â^'yAyO3â^'y/2 (A = Y, Yb, In). Inorganics, 2014, 2, 16-28.	2.7	6
68	5	Investigation into the effect of Si doping on the performance of Sr1â^'yCayMnO3â^'δ SOFC cathode materials. Dalton Transactions, 2013, 42, 5421.	3.3	23
60		Topochemical modifications of mixed metal oxide compounds by low-temperature fluorination routes. Reviews in Inorganic Chemistry, 2013, 33, 105-117.	4.1	61
67	7	A neutron diffraction study and mode analysis of compounds of the system La1â^'xSrxFeO3â^'xFx (x=1,) Tj ETQq1 206, 158-169.		.4 rgBT /Ove 36
68	8	Synthesis, structural and magnetic characterisation of the fluorinated compound 15R-BaFeO2F. Journal of Solid State Chemistry, 2013, 203, 218-226.	2.9	23
69	9	Facile proton conduction in H+/Li+ ion-exchanged garnet-type fast Li-ion conducting Li5La3Nb2O12. Journal of Materials Chemistry A, 2013, 1, 13469.	10.3	57
70		Synthesis, conductivity and structural aspects of Nd3Zr2Li7â^3xAlxO12. Journal of Materials Chemistry A, 2013, 1, 14013.	10.3	25
71	1	Investigation into the effect of Si doping on the performance of SrFeO3â^δSOFC electrode materials. Journal of Materials Chemistry A, 2013, 1, 11834.	10.3	53
72	2	On the soft magnetic properties of the compounds of the series NaxMn4.5â^'x/2(VO4)3 and the magnetic structure of h.tMn3(VO4)2 (x = 1). Dalton Transactions, 2013, 42, 7894.	3.3	4

#	Article	IF	CITATIONS
73	Crystallographic Correlations with Anisotropic Oxide Ion Conduction in Aluminum-Doped Neodymium Silicate Apatite Electrolytes. Chemistry of Materials, 2013, 25, 1109-1120.	6.7	18
74	Battery and solid oxide fuel cell materials. Annual Reports on the Progress of Chemistry Section A, 2013, 109, 396.	0.8	8
75	Synthesis, structural and magnetic characterisation of the fully fluorinated compound 6H–BaFeO2F. Journal of Solid State Chemistry, 2013, 198, 262-269.	2.9	29
76	Oxygen Migration in Dense Spark Plasma Sintered Aluminumâ€Doped Neodymium Silicate Apatite Electrolytes. Journal of the American Ceramic Society, 2013, 96, 3457-3462.	3.8	2
77	Effect of Ga incorporation on the structure and Li ion conductivity of La3Zr2Li7O12. Dalton Transactions, 2012, 41, 12048.	3.3	96
78	Synthesis and Characterization of Oxyanionâ€Đoped Cobalt Containing Perovskites. Fuel Cells, 2012, 12, 1056-1063.	2.4	28
79	Dense Oxide Ion Conducting Apatites Prepared by Spark Plasma Sintering. Proceedings of the National Academy of Sciences India Section A - Physical Sciences, 2012, 82, 43-48.	1.2	5
80	Synthesis and characterisation of vanadium doped alkaline earth lanthanum germanate oxyapatite electrolyte. Journal of Materials Chemistry, 2012, 22, 2658-2669.	6.7	6
81	Insight into the local structure of barium indate oxide-ion conductors: An X-ray total scattering study. Dalton Transactions, 2012, 41, 50-53.	3.3	19
82	Synthesis of new Mn/Ti containing perovskites and examination of their potential for use as solid oxide fuel cell electrodes. International Journal of Low-Carbon Technologies, 2012, 7, 60-62.	2.6	4
83	Synthesis and characterisation of oxyanion-doped manganites for potential application as SOFC cathodes. Journal of Materials Chemistry, 2012, 22, 8287.	6.7	44
84	Synthesis and characterization of proton conducting oxyanion doped Ba2Sc2O5. Dalton Transactions, 2012, 41, 261-266.	3.3	22
85	Battery and solid oxide fuel cell materials. Annual Reports on the Progress of Chemistry Section A, 2012, 108, 424.	0.8	12
86	Synthesis of oxyanion-doped barium strontium cobalt ferrites: Stabilization of the cubic perovskite and enhancement in conductivity. Journal of Power Sources, 2012, 209, 180-183.	7.8	35
87	Low temperature fluorination of Sr3Fe2O7â^'x with polyvinylidine fluoride: An X-ray powder diffraction and Mössbauer spectroscopy study. Journal of Solid State Chemistry, 2012, 186, 195-203.	2.9	23
88	Synthesis of silicon doped SrMO3 (M = Mn, Co): stabilization of the cubic perovskite and enhancement in conductivity. Dalton Transactions, 2011, 40, 5599.	3.3	45
89	Local structure investigation of oxide ion and proton defects in Ge-apatites by pair distribution function analysis. Chemical Communications, 2011, 47, 250-252.	4.1	10
90	Apatite germanates doped with tungsten: synthesis, structure, and conductivity. Dalton Transactions, 2011, 40, 3903-3908.	3.3	29

#	Article	IF	CITATIONS
91	Hydrogen storage and ionic mobility in amide–halide systems. Faraday Discussions, 2011, 151, 271.	3.2	41
92	Oxyanion doping strategies to enhance the ionic conductivity in Ba <sub>2</sub> In <sub>2</sub> O <sub>5</sub> . Journal of Materials Chemistry, 2011, 21, 874-879.	6.7	63
93	Conducting solids. Annual Reports on the Progress of Chemistry Section A, 2011, 107, 434.	0.8	2
94	Strategies for the Optimisation of the Oxide Ion Conductivities of Apatiteâ€Type Germanates. Fuel Cells, 2011, 11, 10-16.	2.4	32
95	Novel Aspects of the Conduction Mechanisms of Electrolytes Containing Tetrahedral Moieties. Fuel Cells, 2011, 11, 38-43.	2.4	15
96	Oxygen Defects and Novel Transport Mechanisms in Apatite Ionic Conductors: Combined <sup>17</sup> Oâ€NMR and Modeling Studies. Angewandte Chemie - International Edition, 2011, 50, 9328-9333.	13.8	57
97	Structure and magnetic properties of the cubic oxide fluoride BaFeO2F. Journal of Solid State Chemistry, 2011, 184, 1361-1366.	2.9	44
98	Protonic defects and water incorporation in Si and Ge-based apatite ionic conductors. Journal of Materials Chemistry, 2010, 20, 2766.	6.7	36
99	Crystal chemistry and optimization of conductivity in 2A, 2M and 2H alkaline earth lanthanum germanate oxyapatite electrolyte polymorphs. Solid State Ionics, 2010, 181, 1189-1196.	2.7	15
100	Synthesis and characterisation of the SrxBa1â´'xFeO3â´'y-system and the fluorinated phases SrxBa1â´'xFeO2F. Solid State Sciences, 2010, 12, 1455-1463.	3.2	46
101	Raman spectroscopy studies of apatite-type germanate oxide ion conductors: correlation with interstitial oxide ion location and conduction. Journal of Materials Chemistry, 2010, 20, 2170.	6.7	30
102	Silicon Doping in Ba <sub>2</sub> In <sub>2</sub> O <sub>5</sub> : Example of a Beneficial Effect of Silicon Incorporation on Oxide Ion/Proton Conductivity. Chemistry of Materials, 2010, 22, 5945-5948.	6.7	42
103	Conducting solids. Annual Reports on the Progress of Chemistry Section A, 2010, 106, 429.	0.8	7
104	New Chemical Systems for Solid Oxide Fuel Cells. Chemistry of Materials, 2010, 22, 675-690.	6.7	329
105	Enhancement of the conductivity of Ba2In2O5 through phosphate doping. Chemical Communications, 2010, 46, 4613.	4.1	44
106	Origami: a versatile modeling system for visualising chemical structure and exploring molecular function. Chemistry Education Research and Practice, 2010, 11, 43-47.	2.5	9
107	Combined experimental and modelling studies of proton conducting La1â^'xBa1+xGaO4â^'x/2: proton location and dopant site selectivity. Journal of Materials Chemistry, 2010, 20, 10412.	6.7	12
108	Solid-State Materials for Clean Energy: Insights from Atomic-Scale Modeling. MRS Bulletin, 2009, 34, 935-941.	3.5	27

#	Article	IF	CITATIONS
109	Ionic Conductivity, Structure and Oxide Ion Migration Pathway in Fluorite-Based Bi <sub>8</sub> La <sub>10</sub> O <sub>27</sub> . Chemistry of Materials, 2009, 21, 4661-4668.	6.7	17
110	Conducting solids. Annual Reports on the Progress of Chemistry Section A, 2009, 105, 436.	0.8	1
111	Pseudomorphic 2A→ 2M→ 2H phase transitions in lanthanum strontium germanate electrolyte apatites. Dalton Transactions, 2009, , 8280.	3.3	14
112	Fluorination of perovskite-related phases of composition SrFe1â^'xSnxO3â^'Î′. Journal of Physics Condensed Matter, 2009, 21, 256001.	1.8	13
113	Preparation of high-oxygen-content apatite silicates through Ti-doping: effect of Ti-doping on the oxide ion conductivity. Journal of Materials Chemistry, 2009, 19, 5003.	6.7	16
114	An investigation of the high temperature reaction between the apatiteoxide ion conductor La <sub>9.33</sub> Si <sub>6</sub> O <sub>26</sub> and NH3. Journal of Materials Chemistry, 2009, 19, 749-754.	6.7	20
115	Neutron diffraction structural study of the apatite-type oxide ion conductor, La8Y2Ge6O27: location of the interstitial oxide ion site. Journal of Materials Chemistry, 2009, 19, 7955.	6.7	28
116	Cation ordering in Li containing garnets: synthesis and structural characterisation of the tetragonal system, Li7La3Sn2O12. Dalton Transactions, 2009, , 5177.	3.3	81
117	Fluorination of perovskite-related phases of composition La1â^'xSrxFe1â^'yCoyO3â^'δ. Journal of Physics and Chemistry of Solids, 2008, 69, 2032-2036.	4.0	16
118	Synthesis and structural investigation of a new oxide fluoride of composition Ba2SnO2.5F3·xH2O (xâ‰^0.5). Journal of Solid State Chemistry, 2008, 181, 2185-2190.	2.9	16
119	Interaction of (La1â^'xSrx)1â^'yMnO3–Zr1â^'zYzO2â~'d cathodes and LaNi0.6Fe0.4O3 current collecting layers for solid oxide fuel cell application. Solid State Ionics, 2008, 179, 732-739.	2.7	30
120	Conducting solids. Annual Reports on the Progress of Chemistry Section A, 2008, 104, 414.	0.8	0
121	Atomic-scale mechanistic features of oxide ion conduction in apatite-type germanates. Chemical Communications, 2008, , 715-717.	4.1	75
122	Local Defect Structures and Ion Transport Mechanisms in the Oxygen-Excess Apatite La <sub>9.67</sub> (SiO <sub>4</sub> ) <sub>6</sub> O <sub>2.5</sub> . Chemistry of Materials, 2008, 20, 5055-5060.	6.7	115
123	Effect of oxygen content on the 29Si NMR, Raman spectra and oxide ion conductivity of the apatite series, La8+xSr2â^'x(SiO4)6O2+x/2. Dalton Transactions, 2008, , 5296.	3.3	64
124	Magnetic order in perovskite-related SrFeO <sub>2</sub> F. Journal of Physics Condensed Matter, 2008, 20, 215207.	1.8	37
125	Conducting solids. Annual Reports on the Progress of Chemistry Section A, 2007, 103, 428.	0.8	2
126	Neutron diffraction and atomistic simulation studies of Mg doped apatite-type oxide ion conductors. Faraday Discussions, 2007, 134, 181-194.	3.2	59

#	Article	IF	CITATIONS
127	Synthesis and structural determination of the new oxide fluoride BaFeO2F. Solid State Communications, 2007, 141, 467-470.	1.9	52
128	Cooperative mechanisms of fast-ion conduction in gallium-based oxides with tetrahedral moieties. Nature Materials, 2007, 6, 871-875.	27.5	185
129	Developing apatites for solid oxide fuel cells: insight into structural, transport and doping properties. Journal of Materials Chemistry, 2007, 17, 3104.	6.7	239
130	Conducting solids. Annual Reports on the Progress of Chemistry Section A, 2006, 102, 482.	0.8	2
131	Solid state 29Si NMR studies of apatite-type oxide ion conductors. Journal of Materials Chemistry, 2006, 16, 1410.	6.7	118
132	A comparison of the effect of rare earth vs Si site doping on the conductivities of apatite-type rare earth silicates. Journal of Solid State Electrochemistry, 2006, 10, 562-568.	2.5	72
133	Fluorination of perovskite-related SrFeO3â~δ. Solid State Communications, 2005, 134, 621-624.	1.9	76
134	Atomic-Scale Investigation of Defects, Dopants, and Lithium Transport in the LiFePO4 Olivine-Type Battery Material. Chemistry of Materials, 2005, 17, 5085-5092.	6.7	966
135	Synthesis and structural characterisation of the new K2NiF4-type phases, A2In0.5Sb0.5O4(A = Sr, Ba). Dalton Transactions, 2005, , 460.	3.3	6
136	Structural studies of apatite-type oxide ion conductors doped with cobalt. Dalton Transactions, 2005, , 1273.	3.3	34
137	24ÂÂConducting solids. Annual Reports on the Progress of Chemistry Section A, 2005, 101, 489.	0.8	6
138	Synthesis and characterisation of the perovskite-related cuprate phases YSr2Cu2MO7+y(M = Co, Fe) for potential use as solid oxide fuel cell cathode materials. Journal of Materials Chemistry, 2005, 15, 2321.	6.7	16
139	Effect of Ba and Bi doping on the synthesis and sintering of Ge-based apatite phases. Journal of Solid State Electrochemistry, 2004, 8, 668.	2.5	25
140	Synthesis and electrical characterisation of the apatite-type oxide ion conductors Nd9.33+xSi6-yGayO26+z. lonics, 2004, 10, 353-357.	2.4	3
141	Development of apatite-type oxide ion conductors. Chemical Record, 2004, 4, 373-384.	5.8	143
142	26 Conducting solids. Annual Reports on the Progress of Chemistry Section A, 2004, 100, 525.	0.8	2
143	Doping and defect association in AZrO3(A = Ca, Ba) and LaMO3(M = Sc, Ga) perovskite-type ionic conductors. Dalton Transactions, 2004, , 3061.	3.3	106
144	Doping strategies to optimise the oxide ion conductivity in apatite-type ionic conductors. Dalton Transactions, 2004, , 3106.	3.3	96

#	Article	IF	CITATIONS
145	Defect chemistry and oxygen ion migration in the apatite-type materials La9.33Si6O26 and La8Sr2Si6O26. Journal of Materials Chemistry, 2003, 13, 1956.	6.7	250
146	An apatite for fast oxide ion conductionElectronic supplementary information (ESI) available: interatomic potentials. See http://www.rsc.org/suppdata/cc/b3/b301179h/. Chemical Communications, 2003, , 1486.	4.1	127
147	25â€ $f$ â€ $f$ Conducting solids. Annual Reports on the Progress of Chemistry Section A, 2003, 99, 477-504.	0.8	2
148	La1â^'xBa1+xGaO4â^'x/2: a novel high temperature proton conductor. Chemical Communications, 2003, , 2694-2695.	4.1	40
149	The Synthesis and Characterisation of Ge Containing Apatite-Type Oxide Ion Conductors. Materials Research Society Symposia Proceedings, 2002, 756, 1.	0.1	Ο
150	La2MgGeO6: a novel Ge based perovskite synthesised under ambient pressure. Chemical Communications, 2002, , 1776-1777.	4.1	14
151	26â€fâ€fConducting solids. Annual Reports on the Progress of Chemistry Section A, 2002, 98, 505-529.	0.8	Ο
152	Synthesis and structure of the new oxide fluoride Sr2TiO3F2 from the low temperature fluorination of Sr2TiO4: an example of a staged fluorine substitution/insertion reaction. Journal of Materials Chemistry, 2002, 12, 291-294.	6.7	53
153	Synthesis and conductivities of the apatite-type systems, La9.33+xSi6â^'yMyO26+z (M=Co, Fe, Mn) and La8Mn2Si6O26. Ionics, 2002, 8, 149-154.	2.4	78
154	An investigation of the synthesis and conductivities of La-Ge-O based systems. Ionics, 2002, 8, 155-160.	2.4	49
155	Synthesis and structure of the new oxide fluoride Ba2ZrO3F2·xH2O (x â‰^0.5). Journal of Materials Chemistry, 2001, 11, 2035-2038.	6.7	29
156	Synthesis and thermal stability of the new copper oxide carbonate Ba4ScCu2O7â^'xCO3 and other members of the series Ba4ScxCu2Oy(CO3)2â^x. Journal of Materials Chemistry, 1999, 9, 545-548.	6.7	3
157	Synthesis and electrical characterisation of doped perovskite titanates as potential anode materials for solid oxide fuel cells. Journal of Materials Chemistry, 1997, 7, 2495-2498.	6.7	157
158	Fluorination of the Ruddlesden–Popper type cuprates, Ln2â^'xA1+xCu2O6â^'y (Ln=La, Nd; A=Ca, Sr). Journal of Materials Chemistry, 1997, 7, 2077-2083.	6.7	20
159	Synthesis and electrical characterisation of the perovskite niobate-titanates, Sr1â^'x/2Ti1â^'xNbxO3â^'δ. Ionics, 1996, 2, 213-216.	2.4	33
160	Cation Distribution and Magnetic Interactions in Substituted Iron-Containing Garnets: Characterization by Iron-57 Mössbauer Spectroscopy. Journal of Solid State Chemistry, 1996, 122, 118-129.	2.9	10
161	Analysis of oxyanion (BO 3 3? , CO 3 2? , SO 4 2? , PO 4 3? , SeO 4 4- ) substitution in Y123 compounds studied by X-ray photoelectron spectroscopy. Journal of Superconductivity and Novel Magnetism, 1996, 9, 97-100.	0.5	39
162	X-ray emission and photoelectron spectra, and the location of fluorine atoms in strontium and calcium copper oxyfluorides. Journal of Physics Condensed Matter, 1996, 8, 4847-4854.	1.8	10

#	Article	IF	CITATIONS
163	Electronic structure of cuprates containing sulfur and phosphorus oxyanions. Physical Review B, 1995, 52, 11830-11836.	3.2	2
164	Chapter 24. Conducting solids, covering ionic and electronic conductors. Annual Reports on the Progress of Chemistry Section A, 1995, 92, 433.	0.8	1
165	Synthesis and structure of the calcium copper oxyfluoride, Ca2CuO2F2+?. Journal of Materials Chemistry, 1995, 5, 913.	6.7	32
166	Chapter 25. Conducting solids, covering ionic and electronic conductors. Annual Reports on the Progress of Chemistry Section A, 1994, 91, 467.	0.8	0
167	Powder neutron diffraction study of the nasicon-related phases NaxMIIxMIII2 –x(SO4)3 –y(SeO4)y: MII= Mg, MIII= Fe, In. Journal of Materials Chemistry, 1994, 4, 1469-1473.	6.7	12
168	Neutron diffraction structural study of the nasicon-related phases LixMIIxMIII2 –x(SO4)3 –y(SeO4)y(MII= Mg, Ni, Zn; MIII= Al, Cr). Journal of Materials Chemistry, 1994, 4, 1463-1467.	6.7	12
169	Oxy-anion substitutions in the system [Y/Ce]2Sr2–xBaxCu3O9–y. Journal of Materials Chemistry, 1993, 3, 1327-1328.	6.7	7
170	Chapter 24. Conducting solids, covering ionic and electronic conductors. Annual Reports on the Progress of Chemistry Section A, 1993, 90, 433.	0.8	0
171	A neutron diffraction study of the system Y1-yCayBa2-yLayCu3O7-x. Superconductor Science and Technology, 1992, 5, 205-209.	3.5	42
172	Synthesis and conductivity of new lithium-containing Nasicon-type phases: Lix[MxIIM2 –xIII](SO4)3 –y(SeO4)yand Lix[Lix/2M2 –x/2III](SO4)3 –y(SeO4)y. Journal of Materials Chemistry, 1992, 2, 1267-1269.	6.7	6
173	Synthesis and structure of Ba4CaCu2.24O6.96(CO3)0.5, a perovskite containing carbonate anions, and related phases. Journal of Materials Chemistry, 1991, 1, 17.	6.7	37
174	The structural effects of Na and Ca substitutions on the Y site in YBa2Cu3O7-x. Superconductor Science and Technology, 1989, 2, 5-8.	3.5	40